Chapter 8

Hybrid Silicon-Organic Heterojunction Structures for Photovoltaic Applications

Andrey Kosarev, Ismael Cosme,
Svetlana Mansurova, Antonio J. Olivares and
Hiram E. Martinez

Additional information is available at the end of the chapter

http://dx.doi.org/10.5772/67565

Abstract

The concept for inorganic-organic device is an attractive technology to develop devices with better characteristics and functionality due to the complementary advantages of inorganic and organic materials. This chapter provides an overview of the principal requirements for organic and inorganic semiconductor properties and their fabrication processes and focus on the compatibility between low temperature plasma enhanced chemical vapor deposition (PECVD) and polymer organic materials deposition. The concept for inorganic-organic device was validated with the fabrication of three hybrid thin film photovoltaic structures, based on hydrogenated silicon (Si:H), organic poly(3-hexythiophene): methano-fullerenephenyl-C61-butyric-acid-methyl-ester (P3HT:PCBM), and poly(3,4 ethylenedioxythiophene): poly(4-styrenesulfonate) (PEDOT:PSS) films. Optoelectronic characteristics, performance characteristics, and interfaces of the different configurations aspects are discussed. Hybrid ITO/PEDOT:PSS/(i)Si:H/(n)Si:H structure results in a remarkably high short circuit current density as large as 17.74 mA/cm^2, which is higher than the values in organic or inorganic reference samples. Although some hybrid structures demonstrated substantial improvement of performance, other hybrid structures showed poor performance, further R&D efforts seem to be promising, and should be focused on deeper study of organic materials and related interface properties.

Keywords: organic semiconductors, plasma deposited materials, thin film devices, hybrid devices, solar cells

1. Introduction

Polymer-based organic semiconductors have attracted considerable attention due to their excellent light absorption properties and compatibility with the solution processing technologies enabling new approaches to fabricate cost-effective, organic thin-film solar cells by printable process. On the other hand, hydrogenated silicon (Si:H) prepared by plasma enhanced chemical vapor deposition (PECVD) is a widely known inorganic semiconductor with rather mature deposition technology, which has been successfully implemented in several commercial optoelectronic devices, including photovoltaics. Important advantages of Si:H and related semiconductors are their high photocarrier generation, good transport properties of photocarriers, possibility to vary optical gap in the range of 1.2–3 eV, and acceptable stability under sun irradiation. Organic solar cells based on conjugated polymers as electron-donor materials blended with small molecule sensitizer as an electron acceptor have achieved 7–9% conversion efficiency in small area single bulk heterojunction devices. The efficiency of single-junction Si:H solar cells is around 10% even with optimal optical design. A few attempts have been undertaken to merge the beneficial properties of both materials in the so-called hybrid silicon-organic heterojunction solar cells. The main idea behind this concept is based on the possibilities to enhance photovoltaic performance characteristics by engineering suitable material and improving interface properties and design. Rather developed deposition and doping process of amorphous silicon and related thin films (intrinsic and p-n-doped) allow to tune the important structural and electronic parameters (such as degree of order, optical gap, mobility, Fermi level position, etc.) of the material which determines the device performance characteristics. Thus, the combination of organic and inorganic materials would be a promising approach for developing new types of large area, lightweight, thin film efficient solar cells.

We present a concept for silicon-organic heterojunction structures for photovoltaic devices, based on mainly PECVD noncrystalline silicon (can be also extended and involve crystalline semiconductors) describe fabrication of both plasma deposited films and organic materials and their relevant electronic properties, fabrication of hybrid device structures, and their characteristics comparing with those reported in literature.

2. Fabrication and electronic properties of plasma deposited and organic materials

2.1. Inorganic materials based on silicon deposited by PECVD

Technology based on amorphous silicon semiconductors has become an important part in the multibillion business in electronics in the last decades. There was a time, when the theory of the physical properties of solids seems to be impossible without considering a stable and periodic structure, Ziman [1]. However, nowadays, the theory of amorphous materials has not only been developed but also technology based on these materials has become omnipresent in wide range of electronic applications. The breakthrough of amorphous silicon materials was directly related to the development of a new method called GD that allowed for the first time

http://dx.doi.org/10.5772/67565

to deposit intrinsic hydrogenated amorphous silicon (a-Si:H) films [2, 3] with high photoconductivity and low concentration of ESR centers, p-type and n-type doped amorphous silicon films, Spear and Le Comber [4], with sufficient quality (low DOS) to be used in functional p-n junctions [5].

The modern approach of the GD system used for first time is now well-known (PECVD). The actual PECVD technique has reached the versatility to deposit not only amorphous silicon but also silicon materials in their entire range of structure: nanostructured [6], microcrystalline [7, 8], epitaxial crystalline silicon [9], and alloys such as SiGe:H, SiC:H, SiO:H, SiN:H, etc. The optoelectronic properties of these materials depend on the deposition parameters such as pressure, flow rate, substrate temperature, power, and excitation frequency. Good electronic properties for interesting high Ge-content nanostructured Si_xGe_y:H films deposited at 300°C, high H-dilution ratio, and low frequency have been systematically reported in Ref. [10]. On the other hand, one of the main characteristics of the PECVD technique to take advantage for actual applications is the relative low temperature process in the range of 100–300°C. Low temperature process is a requirement for new applications such as large area, lightweight, flexible devices on low-cost plastic substrates, and, more recently, hybrid organic-inorganic devices based on polymers. It was general to think that reduction of temperature below 200°C leads to the increase of dangling bonds (defects) and results in films with electronic properties that are generally poor [11]. However, it has been found that deterioration of electronic properties in materials deposited at temperature lower than $T < 300$°C can be corrected by other fabrication parameters. Low-temperature (LT) a-Si:H and LT nanocrystalline (nc) Si:H have been optimized at $T = 120$ and 75°C as reported in Ref. [12].

A-Si:H films deposited at reference temperature ($T = 300$°C) show a dark conductivity in the range of 10^{-10} Ω^{-1} cm^{-1} in comparison to LT a-Si:H films that show values of 4×10^{-11} Ω^{-1} cm^{-1} for 120°C and 9×10^{-11} Ω^{-1} cm^{-1} for 75°C, and optical gap parameters were 1.75, 1.92, and 1.90 eV for 300, 120, and 75°C, respectively [12]. The higher optical gap of LT films could be explained for changes in the way that hydrogen is incorporated to the films at low temperatures: 10% for 300°C, 10.9% for 120°C, and 9.5% for 75°C, this effect should be considered for optimization at low temperatures. Intrinsic LT (75°C) nc-Si:H films show a dark conductivity 3×10^{-7} Ω^{-1} cm^{-1}, a crystallinity of 75% and a grain size of ~20 nm, and a doped n^+-doped nc-Si:H film shows a dark conductivity of 0.3 Ω^{-1} cm^{-1}, a crystallinity of 72%, and a grain size of ~15 nm. As reference, a nc-Si:H deposited at 300°C shows a dark conductivity of 10^{-6} Ω^{-1} cm^{-1}, crystallinity of 82%, and a grain size of ~30 nm [12]. For solar cell development, the use of μc-Si:H and a-SiGe:H layers is critical to improve IR long wavelength sensitivity [13]. However, only few systematic studies of the role of temperature on the film growth process and its effect on the film optoelectronic properties have been reported. Modeling of properties for microcrystalline silicon films deposited by PECVD at low temperature (175°C) on flexible low-cost substrate is reported in Ref. [14]. Films under microcrystalline growth conditions with different deposition temperatures for solar cell devices were studied [15]. In Ref. [16], amorphous and microcrystalline silicon films were deposited by RF PECVD at deposition temperatures of 25 and 100°C. Values of properties for μc-Si:H films deposited by RF PECVD were at 25°C: deposition rate $V_d = 0.09$ A°/s, optical gap $E_{opt} = 2.10$ eV, dark conductivity $\sigma_d = 8.6 \times 10^{-9}$ Ω^{-1} cm^{-1}, photoconductivity $\sigma_{ph} = 5.9 \times 10^{-8}$ Ω^{-1} cm^{-1}, and activation energy

E_a = 0.63 eV, and at 100°C: V_d = 0.12 A°/s, E_{opt} = 2.14 eV, $\sigma_d = 3 \times 10^{-5}\ \Omega^{-1}\ cm^{-1}$, $\sigma_{ph} = 1.7 \times 10^{-5}\ \Omega^{-1}\ cm^{-1}$, and E_a = 0.31 eV. On the other hand, a-SiGe films could be an option for application on flexible hybrid solar cells. Deposition of silicon-germanium alloys at low temperatures has been studied since the 1970s [17–20]. The Ge atom is slightly larger and remarkably heavier compared to Si atom, thus changing growth, structure, and consequently electronic properties of Si-Ge:H and Ge:H films. To compensate this, several approaches have been made, such as ion bombardment [21], thickness optimization [22], and hydrogen dilution [23]. Nanostructured high Ge-content GeSi:H films have been studied in [10] (**Figure 1**). These films demonstrated good electronic properties such as low defect and tail state-related absorption (**Figure 2**). Nanostructured $Ge_{0.96}Si_{0.4}$:H films deposited by LF PECVD at deposition temperature T_d = 300°C and high H-dilution ratio R_H = 75 showed a E_{opt} = 0.94 eV, $\sigma_d = 2.5 \times 10^{-4}\ \Omega^{-1}\ cm^{-1}$, and E_a = 0.28 eV. A comparison of the nanostructured $Ge_{0.96}Si_{0.4}$:H film deposited at 300°C and a LT GeSi:H film deposited at 160°C is presented in Ref. [24]. The LT GeSi:H shows a $\sigma_d \sim 10^{-4}\ \Omega^{-1}\ cm^{-1}$ and E_a = 0.32 eV, the absorption coefficient spectra also showed good electronic properties as low defect. **Table 1** shows a summary of electronic properties of silicon-based films deposited by PECVD at high and low temperature. Thus, these results show that high quality silicon materials can be deposited at low temperatures compatible with organic polymer semiconductors deposited on plastic substrates.

2.2. Polymer organic materials

Organic materials based on polymer semiconductors have been in focus during the last decade. The most studied materials such as the bulk heterojunction P3HT:PCBM and the conductive semiconductor PEDOT:PSS have been widely implemented in new organic thin-film solar cells [26]. One important advantage of these materials is their solution type processing techniques for fabrication that allows printable deposition of the films at room temperature and at atmospheric pressure in comparison to inorganic material deposition that usually

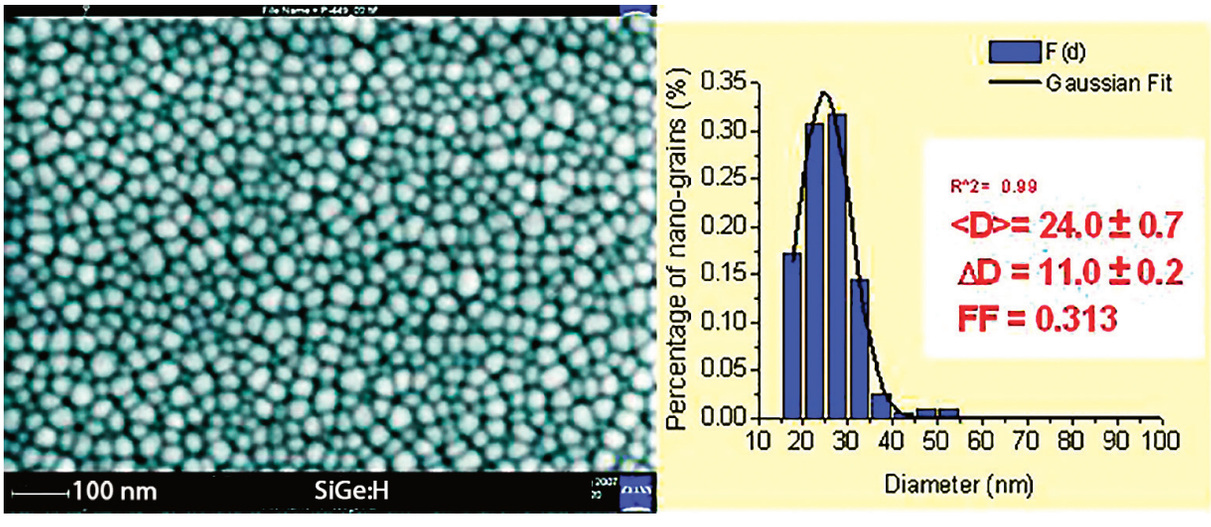

Figure 1. SEM images (left) of nanostructured $Ge_{0.96}Si_{0.4}$:H films deposited by LF PECVD at high H-dilution ratio R_H = 75. Diameter distribution function of grains (right).

http://dx.doi.org/10.5772/67565

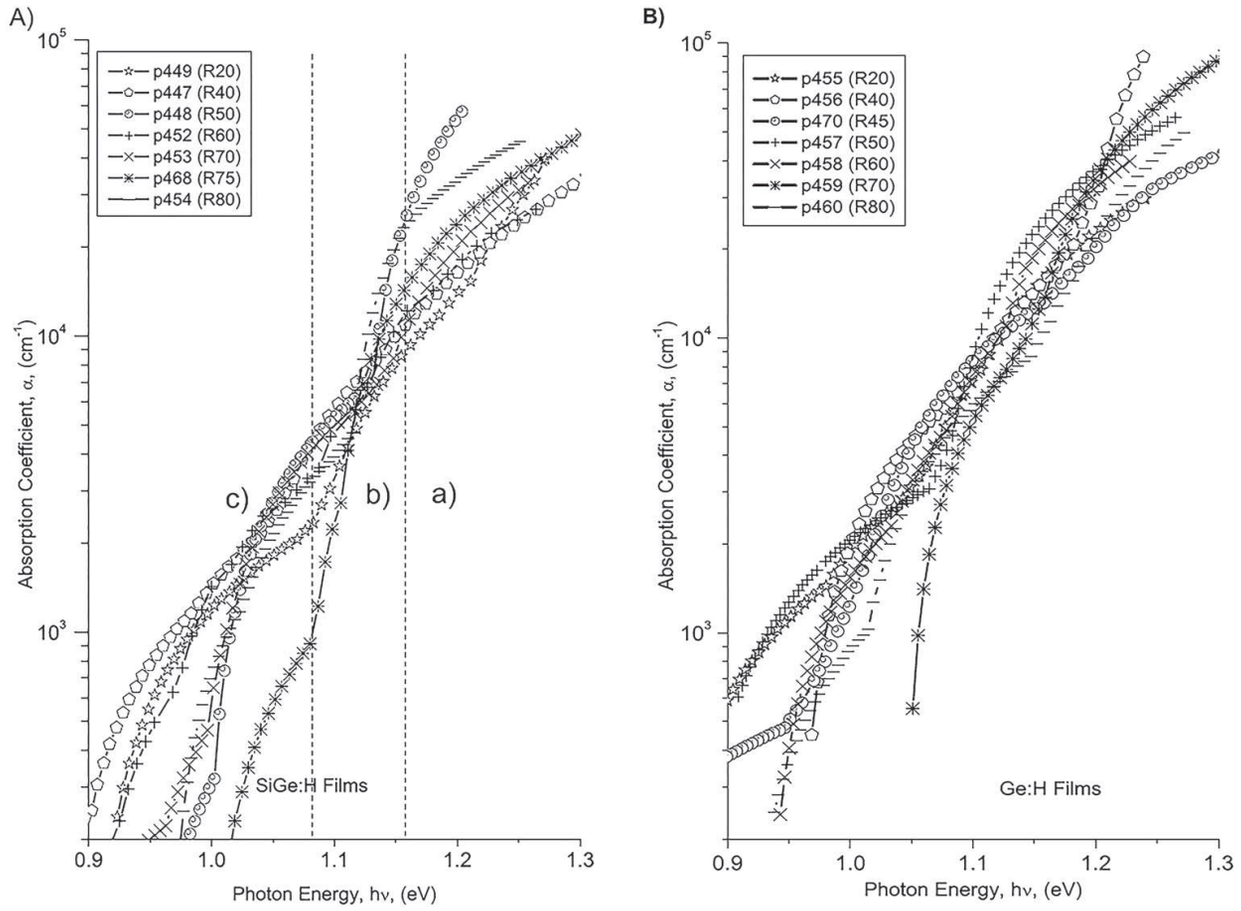

Figure 2. Spectral dependence of optical absorption coefficient $\alpha(h\nu)$for different hydrogen dilution, *R,* (a) SiGe:H and (b) Ge:H films.

Film	Temperature (°C)	V_d (A°/s)	E_{opt} (eV)	σ_d (Ω^{-1} cm^{-1})	σ_{ph} (Ω^{-1} cm^{-1})	E_a (eV)	Other	Ref.
a-Si:H	300	–	1.8	8×10^{-10}	–	0.60	–	[24]
		–	1.75	~10^{-10}	–	–	–	[12]
	220	0.93	1.72	1.1×10^{-9}	1.8×10^{-4}	0.93	RF	[16]
	120	–	1.92	4×10^{-11}	–	–	–	[12]
	75	–	1.90	9×10^{-11}	–	–	–	[12]
nc-Si:H	300	–	–	~10^{-6}	–	–	–	[12]
	75	–	–	3×10^{-7}	–	–	–	[12]
μc-Si:H	100	0.12	2.14	3×10^{-5}	1.7×10^{-5}	0.31	RF	[16]
	25	0.09	2.10	8.6×10^{-9}	5.9×10^{-8}	0.63	RF	[16]
GeSi:H	300	2.2	0.94	2.5×10^{-4}	–	0.28	LF	[10]
	160	1.3	0.95	1.3×10^{-4}	7.5×10^{-6}	0.32	LF	[25]

Table 1. Optoelectronic characteristics comparison for silicon-based films deposited at different temperatures.

requires high substrate temperature and complex high vacuum process. The film-forming processes for organic materials can be classified in (1) coating process methods that include spin coating, blade coating, spray coating, and painting and (2) printing process methods thus include screen printing, offset printing, and inkjet printing [27]. Spin coating method has been one of the important techniques for the deposition of polymer materials. The final characteristics of the films depend on the specific material and its solvent at a given concentration, see, for example, **Figure 3**, it is shown that the thickness dependence as a function of the rotation velocity for PEDOT:PSS films deposited by spin coating at different IPA solvent concentrations. Spin coating deposition is a complex process that also depends among others properties of viscosity, molecular weight, diffusivity, and volatility of the material; however, it is a highly reproducible process [27]. Nevertheless, there are some aspects that limit the application of the technique for industrial production such as no possibility for deposition on large areas, serial production, and problems with patterning. A review of alternatives to spin coating method for the deposition of polymer materials is presented in Ref. [29], just to recognize that the "ideal" process for the deposition of organic materials is still unresolved and an urgent task for the future of this technology.

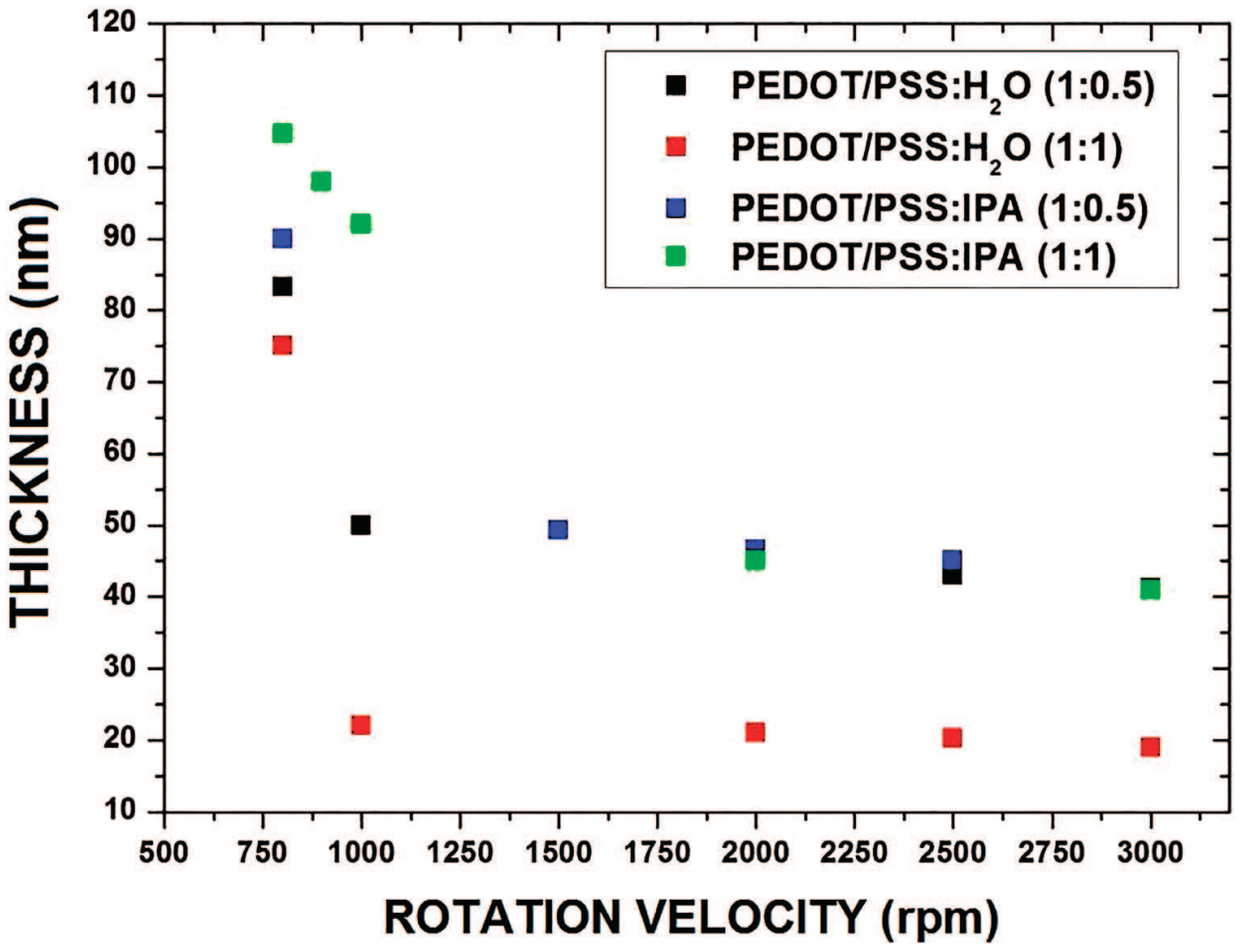

Figure 3. Deposited thickness of PEDOT:PSS films deposited by spin coating as function of frequency rotation for different dilution preparation.

http://dx.doi.org/10.5772/67565

Despite the large number of developed organic materials, there are a few materials that have been usefully applied in promising optoelectronic devices, i.e., PEDOT:PSS is a very attractive conductive polymer semiconductor for electronic and photovoltaic applications (not only for organic electronics) due to its optical transparency, high conductivity, and processing techniques. The use of PEDOT:PSS in hybrid organic-inorganic solar cells and devices has attracted the attention in recent years specially as a candidate for substitution of p-type a-SiC:H:B layer in silicon-based photovoltaic devices [28–30]. The Si/PEDOT interface has shown interesting properties such as effective formation of blocking barrier for electrons, acting similar to an "ideal" barrier [29]. Other advantage of PEDOT:PSS versus traditional inorganic p-type a-Si:H is the flexibility of processing; **Figure 4** shows the DC conductivity, $\sigma_{DC}(T)$, for the spin-coated PEDOT:PSS films deposited under different dilutions. A change in room temperature conductivity of one order of magnitude is obtained only with a change in concentration of dilution with isopropyl alcohol (IPA) [32]. This process seems to be simple in comparison to the required doping process for inorganic semiconductors. However, despite the application of PEDOT:PSS in structures and devices, only a few studies of the electrical properties has been performed. Organic materials are following similar history to amorphous semiconductors, where the practical applications were growing faster than the development of theoretical physics of the materials. In [31],

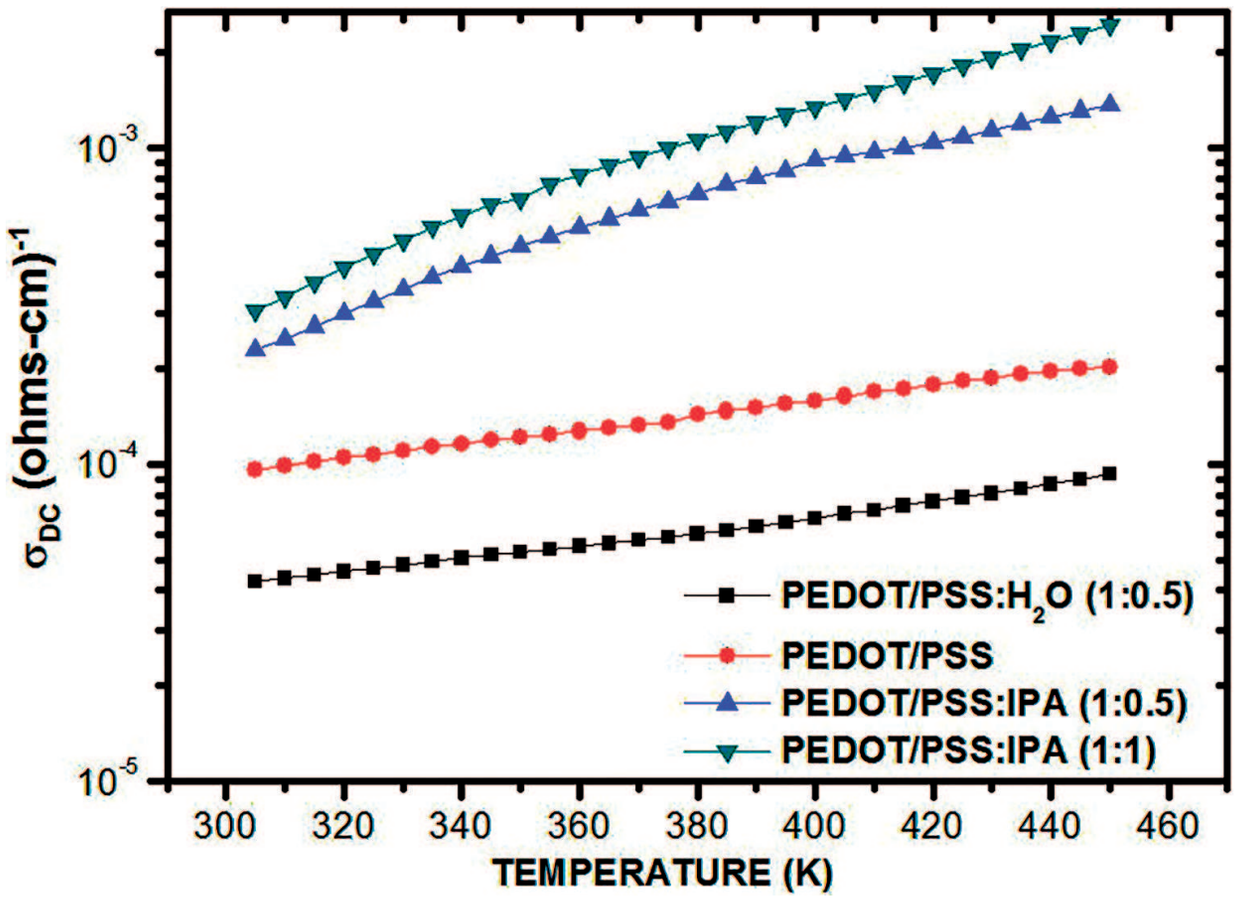

Figure 4. DC conductivity, $\sigma_{DC}(T)$, for the spin-coated films: PEDOT/PSS: H_2O (1:0.5), PEDOT:PSS (without dilution), PEDOT/PSS: isopropyl alcohol (IPA) (1:0.5), and PEDOT/PSS:IPA (1:1) from 300 to 440 K.

the temperature dependence of DC conductivity of spin-coated poly PEDOT:PSS films has been investigated, $\sigma_{DC}(T)$ was measured in films deposited from different mixtures of PEDOT:PSS (**Figure 4**). Experimental data was fitted with two different transport models: thermal activated conduction and variable range hopping (VRH) model. It was found that $\sigma_{DC}(T)$ of PEDOT:PSS/IPA (1:1) sample can be described by the one-dimensional (1D) VRH model; however, at least at below room temperature it is not possible to distinguish unambiguously a concrete model from these two. The versatility of organic materials allows different functions to realize with the same material. PEDOT:PSS has been studied also as replacement of transparent contact oxides (TCO) as it will be discussed in the next section.

2.3. Transparent contact issues

For several years, TCOs were a unique option used as transparent contacts in optoelectronic applications due to their transparency in visible range ($0.4 < \lambda < 0.7$ μ) and low resistivity ($R_{sq} < 100$ Ω/sq). TCOs can be deposited as thin films by techniques as chemical vapor deposition, pulsed laser deposition, spray pyrolysis, and sputtering. There are many studies with a wide background about the development of this technology and film properties [32]. However, to fabricate transparent contacts compatible with the new hybrid inorganic-organic technology and/or compatible with flexible substrates, it is necessary to achieve good optoelectronic properties at low process temperatures (<200°C). To reach this goal, the following approaches have been proposed: (1) to modify the standard deposition methods, (2) to propose new techniques of deposition, or most recently (3) to propose new materials with fabrication methods at room temperature, i.e., organic-based materials. Sputtering method has been modified to achieve TCOs with high optical transmittance and low resistivity at low temperature deposition. ITO (In_2O_3) films deposited by roll-to-roll sputtering at low substrate temperature <50°C show sheet resistance of 47.4 Ω/sq. and a transmittance of 83% [33]. On the other hand, AZO films have been extensively studied as alternative to ITO films due to their stability, high transmission, high conductivity, lower cost, and lower deposition temperature in comparison to ITO films (AZO films, R_{sq} ~ 8.5 Ω/sq and T_{avg} = 84.44% @ T_d = 200°C on glass) [34]. In [35], ZnO/Al (AZO) films were codeposited using pulsed-direct current (DC)-magnetron reactive sputtering processes at 188°C using "soft power." The obtained ZnO:Al films show a sheet resistance of about R_{sq} ~ 13 Ω/sq and a transmittance of ~85%.

Recently with the introduction of organic materials and new technologies, new options have been studied for substitution of traditional TCOs to overcome some disadvantages as low transmission in blue region, high cost, complex high vacuum process, mechanical characteristics, and scarcity. To achieve this, here are some proposals: thin film grids [36], high carbon-based materials [37], and organic polymers [38–40]. PEDOT:PSS has been one of the most investigated organic materials as alternative to TCOs, the polymer has shown higher transparency and conductivity than traditional ITO contacts. Additionally, PEDOT:PSS can be deposited by dispersion in water which is compatible with large area, flexible, and low-cost substrates [41]. The electrical conductivity of PEDOT:PSS can be increased by orders of magnitude using secondary "dopants" as solvents, polyols, surfactants, among others [42]. By solvent dilution and post-treatment method the conductivity of PEDOT:PSS films has reached values of 1418 Ω^{-1} cm^{-1}, low sheet resistance below 65 Ω/□, and transmission

in visible range >80%, which have been reported in [38]. In Ref. [43], silver nanostructures were used to enhance conductivity of PEDOT:PSS contacts using a codeposition of spray and inject printing techniques, and the lower sheet resistance achieved by this method was 26.2 Ω^{-1} cm^{-1} with an average transmission of 80.7%.

2.4. Flexible substrates issues

Hybrid inorganic-organic devices seem to be an attractive approach for large area, lightweight flexible solar cells. Flexible electronics also opens the landscape to new applications such as flexible displays, X-ray sensors, electronic textiles, and electronic skin [42]. Many materials have been investigated as flexible substrates: thin glass substrates [44], metal foils [45], and different polymeric films (PET, PEN, Polyimide – KAPTON®, etc.) [41]. The substrate-specific requirements depend strongly of the application, process fabrication, and technology: optical properties, surface roughness, thermal properties, chemical properties, mechanical properties, and electrical and magnetic properties [12]. In the case of applications in organic hybrid solar cells, special attention should be paid to thermal properties, optical properties, and surface roughness. **Table 2** presents a comparison of the main properties of flexible substrates. One of the most attractive materials for their flexibility, low cost, and transparency are the plastic substrates. **Figure 5** shows the spectral dependence of the optical transmittance in the visible range of plastic substrates. PEN and PET are most desirable materials for solar cells application due to the optical transmittance and relative low cost. Another interesting material is PTFE or TEFLON®; the comparison of transmittance spectra presented in **Figure 5** shows that TEFLON transparent thin film is an attractive candidate for application in solar cell application with transparency from 250 to 900 nm and high transmittance (~96%) of above 350 nm. However, TEFLON has a nonpolar surface or a relative low surface energy to the polymer and inorganic materials, which result in low adhesion [46]. Polymer substrates require relatively low processing temperature, below T = 250°C, in the case of both technologies, organic and PECVD Si-based materials, for fabrication of hybrid solar cells. In both technologies, several approaches have been developed for fabrication of flexible devices like PECVD roll-to-roll fabrication. Inorganic PECVD materials have a long history in this field [12]. However, flexible plastic substrates despite having a scope of challenges are very attractive for large-area scale, lightweight, and relatively low cost hybrid organic-inorganic devices.

Substrate	Temperature process (°C)	Transparency (%)	Flexibility	Planarization
Thin glass	600	Yes	Some	No
Metal foil	1000	No	Some	Yes
Polyamide	<300	Some	Yes	No
PEN	<180	Yes	Yes	No
PET	<120	Yes	Yes	Maybe
TEFLON	<240	Yes	Yes	Maybe

Table 2. Comparison of substrate properties for solar cell applications [12, 25].

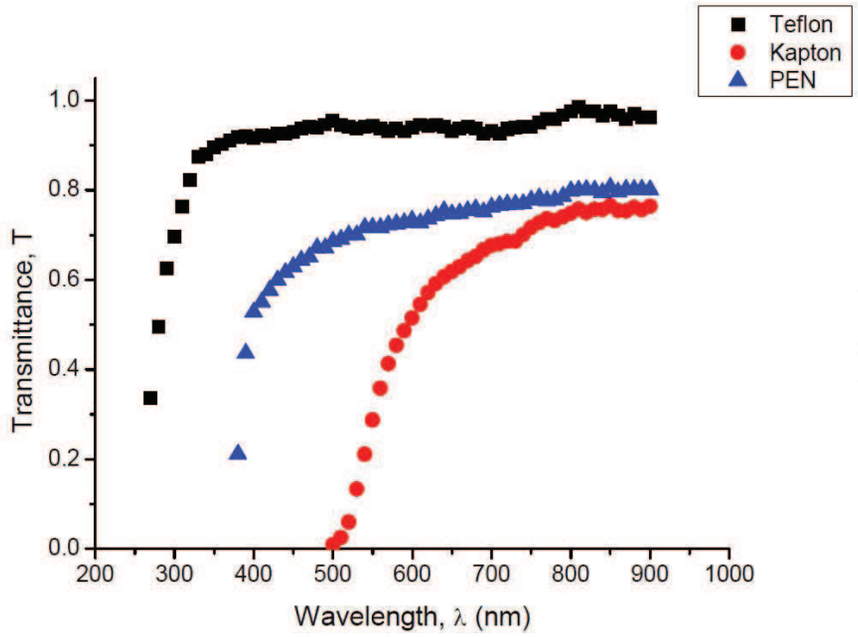

Figure 5. Spectral dependence of optical transmittance for TEFLON, KAPTON, and PEN.

3. Concept for inorganic-organic hybrid device structure

3.1. Concept

A concept for inorganic-organic device (CIOD) structures can be developed taking into account the following material aspects: (a) compatibility of deposition technologies for inorganic-organic semiconductors and electrode materials, (b) complementary of electronic properties of these materials resulting in improvement of device performance, and (c) some technological advantages in device fabrication, e.g., organic materials can be deposited by printable PC controlled technique resulting in simplification of patterning. Inorganic semiconductors can be presented by both crystalline materials and PECVD noncrystalline materials. The latter is applicable for large area flexible devices. In general, CIOD includes various combinations of crystalline and noncrystalline materials together with organic materials. In our further consideration, we shall be focused on PV applications based on PECVD films and organic materials because of their promise for large area flexible devices, although for achieving very high efficiency more complex (crystalline inorganic)-(noncrystalline inorganic)-(organic) material combinations would be of much interest.

3.2. Strategies for CIOD structures aimed at performance improvement

Performance of PV device is determined by: (a) generation of photo-induced carriers controlled by light absorption, (b) transportation of photo-induced carriers controlled by built-in electric field and diffusion, (c) life time of photocarriers that determine both concentration and transport of photocarriers, and (d) properties of interfaces, which control generation-recombination near interface and charge transport through the interface. We select p-i-n configuration as basic PV device structure, where p-layer is p-doped semiconductor, i-layer is intrinsic (nondoped)

http://dx.doi.org/10.5772/67565

semiconductor, and n-layer is n-type semiconductor. Internal built-in electric field in this structure is created because of difference in work functions for p- and n-layer. PECVD silicon is conventionally used as intrinsic semiconductor (nondoped), boron-doped as p-layer and phosphor-doped as n-layer. Optical gap for Si:H is typical E_{opt} = 1.7 eV. PECVD materials allow changes in optical gap and consequently spectral absorption in a wide range. To improve optical absorption in short wave range, PECVD silicon-carbon alloys SiC:H are used with optical gap E_{opt} up to 2.5 eV. For long wave range, PECVD silicon-germanium alloys are used with optical gap as low as E_{opt} = 1.2 eV. Interface properties in the structures even prepared in PECVD cluster tool systems depend strongly on process fabrication and deposition regimes used. Let us analyze the above-mentioned principal factors one by one and start with the increase of effective optical absorption in device structure. The latter can be obtained by means of bi-layer (inorganic-organic) absorber of nondoped materials. In this case, organic material typically with wider band gap than Si:H could improve absorption in short wave range. For improvement of absorption in long wave range, SiGe:H layer could be added. To improve transport of photocarrier in organic nondoped materials, built-in electric field can be formed by means of p- and n-doped PECVD films. It is well known, that device performance in shortwave range depends critically on frontal interface (usually it is p-i interface). Improved photocarrier collection for shortwave have been reported for interfaces with organic p-layer [28, 29]. On the other hand, organic semiconductor with narrow band gap have not sufficiently developed yet, therefore, long wave absorption can be improved by incorporation of SiGe:H films. Some of these ideas have been realized and their fabrication and characterization will be described further.

Most of mature solar cell technologies are being developed with silicon-based materials. The stability with sufficient efficiency of these solar cells has been demonstrated for several years. However, in comparison to new thin film organic materials, they have complex fabrication process, high relative cost, and do not suit well for large area flexible PV devices. New technologies such as organic polymer materials bring new approaches of fabrication techniques and materials that can be molecular designed and tailored with specific optoelectronic properties but efficiency and stability are relatively low in comparison to inorganic counterpart. Thus, the combination of both technologies is looking for devices that can take advantage of the strong optical absorption of organic polymer materials, high charge carrier mobility, and stability of inorganic materials while looking for simplification of process fabrication. Different approaches have been proposed to combine both technologies, the versatility of organic materials results in many possibilities for forming hybrid devices structures [47]. Silicon remains a good candidate for hybrid devices due to favorable and well-known electronic properties. Different ways have been reported to combine silicon with polymers in hybrid solar cell: hybrid crystalline silicon-PEDOT:PSS solar cell [29], nanowire-Si/polymer solar cells [48], and a-Si:H/PEDOT:PSS pin solar cell [28]. **Figure 6** shows examples of some ideas for application of organic and inorganic materials in hybrid solar cells. In the structure labeled H1 with configuration (ITO)(p) SiC:H/P3HT:PCBM/(n) Si:H), P3HT:PCBM bulk heterojunction film is used as active absorber film and conventional a-Si:H and a-SiC:H are used as n-type and p-type layers, respectively. The structure labeled H2 (ITO/PEDOT:PSS/(i) Si:H/(n) Si:H) is an a-Si:H p-i-n structure, where the p-type SiC:H layer was substituted by an organic conductive film (PEDOT:PSS). Finally, the structure labeled H3 is a double-absorber layer structure (ITO/PEDOT:PSS/P3HT:PCBM/(i) Si:H/(n) Si:H).

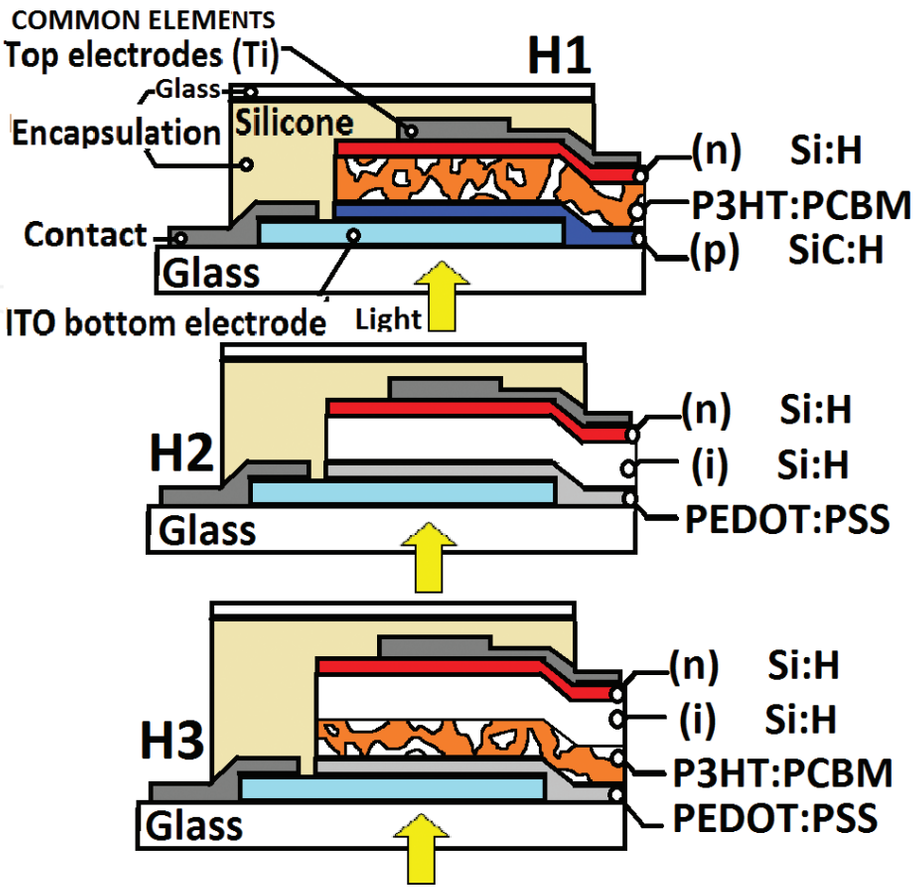

Figure 6. Hybrid photovoltaic structures based on Si:H and organic semiconductors (H1) ITO/(p) SiC:H/P3HT:PCBM/(n) Si:H, (H2) ITO/PEDOT:PSS/(i) Si:H/(n) Si:H, and (H3) ITO/PEDOT:PSS/P3HT:PCBM/(i) Si:H/(n) Si:H.

3.3. On electron energetical diagrams for hybrid device structures

Electron energetic diagram is a conventional and convenient instrument applied to the analysis of device structures and their performance. Such diagram can be created if electronic properties (optical gap, work function, electron affinity, etc.) are known (well measured) that does not exist even in crystalline semiconductors. Moreover, knowledge of bulk electronic characteristics is not sufficient because information on interfaces is required as well. As far as organic semiconductors are concerned, data reported on bulk electronic properties are very poor and those for interfaces have not been reported. In many publications, "energetic diagrams" look as a set of energetic sketches for different materials with different Fermi levels and some arrows denoted hypothetical electron transitions. This is misleading because in multilayered device structure without illumination a thermal equilibrium is suggested (i.e., exchange of particles and their energies between materials) meaning the same Fermi level in the system, rather than different ones in isolated materials. Under illumination, electronic diagram becomes significantly more complex and can only be created based on special experimental study of device structure. Nevertheless, design of energetic diagram based on available experimental data (even with some shortages and errors in details) is strongly motivated. In **Figure 7**, such hypothetical electron energetic diagrams in thermal equilibrium for H1,

http://dx.doi.org/10.5772/67565

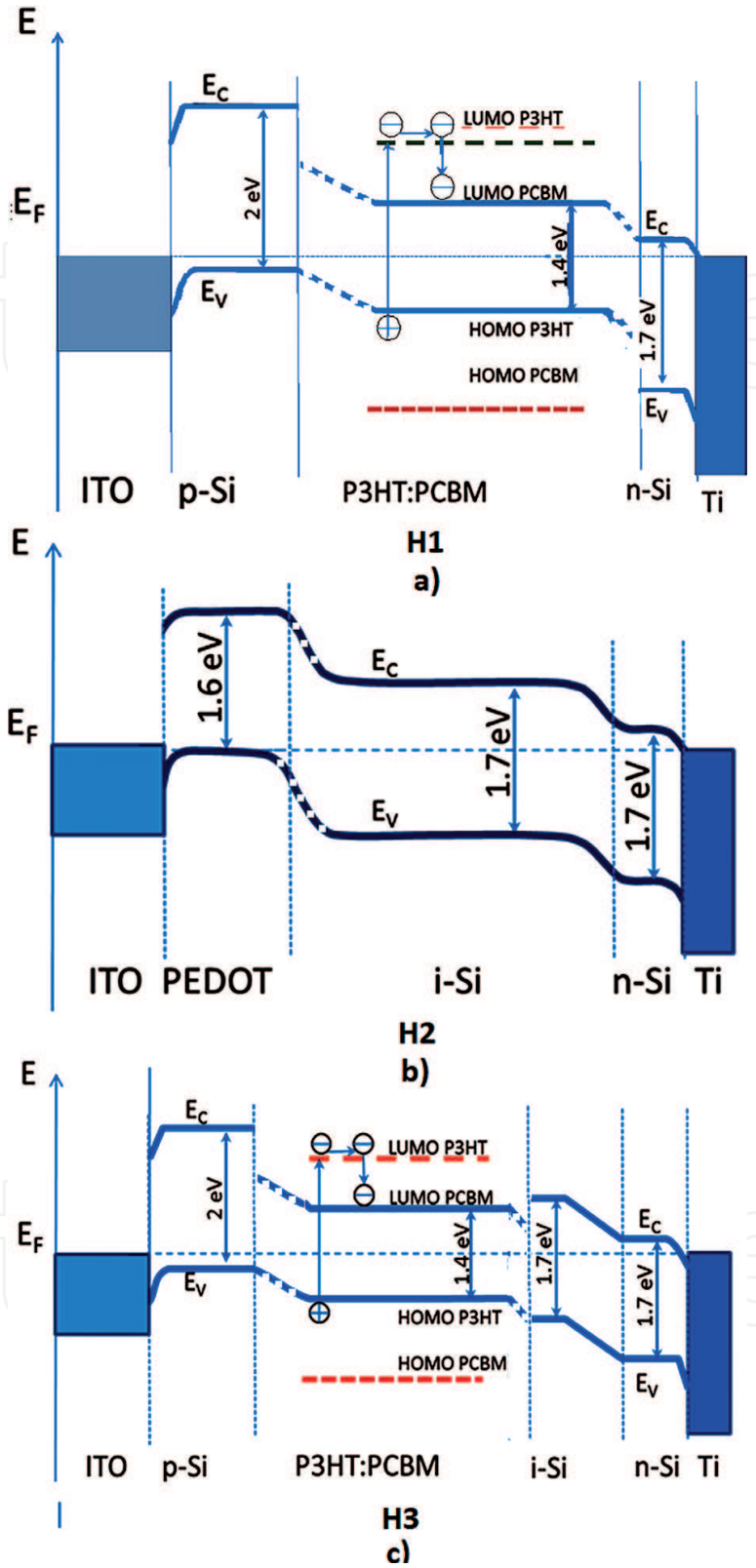

Figure 7. Electron energetic diagrams in thermal equilibrium for the studied structures: (a) ITO/(p) SiC:H/P3HT:PCBM/(n) Si:H (H1), (b) ITO/PEDOT:PSS/(i) Si:H/(n) Si:H (H2), and (c) ITO/PEDOT:PSS/P3HT:PCBM/(i) Si:H/(n) Si:H (H3). Dotted lines represent hypothetical interfaces and offsets in the energy levels due to lack of information on the values reported in literature.

H2, and H3 structures are represented, more details about them can be found in Ref. [28]. In H1, energetic diagram (**Figure 7a**) shows that the light absorption occurs in the organic bulk heterojunction formed by P3HT and PCBM. The creation of an exciton (bounded electron-hole pair) in P3HT is followed by separation of the charge at the internal interfaces of the heterojunction P3HT/PCBM. The inorganic p- and n-type silicon-based layers are used to create an internal electrical field to transport the "free" charge to electrodes. In H2 structure the PEDOT:PSS layer acts as a heavily doped p-type layer and its comparable optical gap (~1.6 eV) to amorphous silicon (~1.7 eV) forms an optimal internal build-in-field and prevents back diffusion of electrons at the frontal interface. In H3 structure improvement of light absorption is expected by using double active absorber layers (a-Si:H and P3HT:PCBM), the energetic diagram shows that one obstacle of this is that the alignment of energetic band between organic and inorganic materials is complex and may create barriers, which oppose to electron and hole transport.

4. Experimental results on fabrication and characterization of different configurations of silicon-organic p-i-n heterojunction structures

4.1. Fabrication

The fabrication flow chart for the H2 structure (ITO/PEDOT:PSS/(i) Si:H/(n) Si:H) is shown in **Figure 8**. The process begins with a coated ITO substrate. The bottom electrode was defined by etching using hydrochloric acid and then the substrate is cleaned by ultrasonic cleaning in acetone and then isopropyl alcohol. The PEDOT:PSS solution was prepared with a 1:6 weight ratio, filtered using a pore size filter of 0.45 μm and deposited by a spin-coating in N_2 ambient with a rotation speed of 2500 rpm that results in a thickness of the film of d = 45 nm. The inorganic layers were deposited by RF PECVD process in a multichamber system. The silicon films were grown by a 10% SiH_4 + 90% H_2 gas mixture for intrinsic film and 0.01% PH_3 + 9.9% SiH_4 + 90.09 % H_2 gas mixtures for n-type layers, at pressures of 550 mTorr and substrate temperature of 160°C. All the gases used were semiconductor purity from "Matheson Inc." The compatibility of PECVD process and organic materials for this flow process has been reported in [25].

4.2. Characterization

Figure 9 shows the DC current density—voltage characteristics J(U) under AM1.5 standard illumination for nonoptimized hybrid structures presented in **Figure 6**. As seen, the structure H1 with organic semiconductor as nondoped intrinsic material demonstrate low U_{OC} = 185 mV, while expected values based on difference of Fermi levels for p- and n-layers could be close to $\Delta E_F \approx 900$ mV. The reduced U_{OC} value may be related to low shunt resistance due to leakage transversal current resulting in low J_{SC} current. Mechanism of leakage current in such structures has not been studied yet and could be rather complex because of the complex structure of the organic material (e.g., see SEM image in **Figure 13**). The highest value of J_{SC} = 5.87 mA/cm^2 is observed in H2 structure with PEDOT/PSS as p-layer and i-Si:H as nondoped absorber and Si:H(P) as n-layer. U_{OC} = 400 mV in this structure is better than in H1 but still

http://dx.doi.org/10.5772/67565

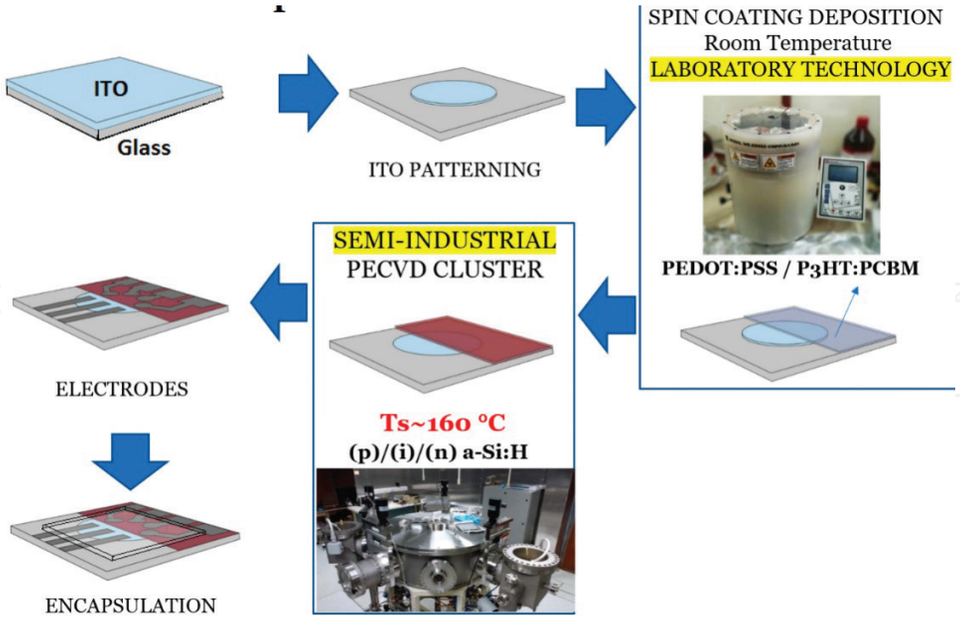

Figure 8. Flow fabrication for thin film silicon/organic p-i-n structure involving PECVD process and spin on coating deposition for inorganic and organic films, respectively.

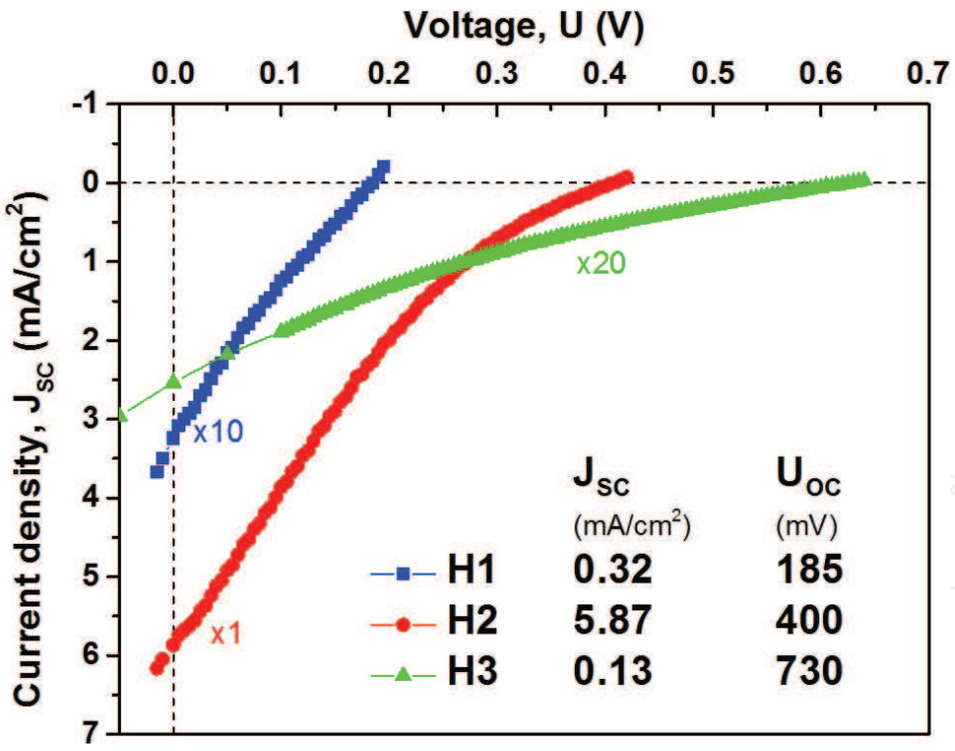

Figure 9. Current-voltage characteristics and extracted *U*oc, J_{SC}, *FF* values of hybrid photovoltaic structures based on Si:H and polymer organic semiconductors (H1) ITO/(p) SiC:H/P3HT:PCBM/(n) Si:H, (H2) ITO/PEDOT:PSS/(i) Si:H/(n) Si:H, and (H3) ITO/PEDOT:PSS/P3HT:PCBM/(i) Si:H/(n) Si:H.

less than that expected. The H2 structure clearly shows current suppression at low internal field, when the potential is close to U_{OC} suggesting still high value of transversal leakage current. The structure with double absorber layer H3 has the highest U_{OC} = 700 mV, but very low

current density J_{SC} = 0.13 mA/cm^2. It means that the structure has sufficient internal electric field but very low current. For speculative purpose, the following reasons of low current can be mentioned: (a) too high resistivity of nondoped organic and inorganic layers, (b) not optimal thicknesses for nondoped layers, and (c) blocking barrier between two nondoped layers. However, special study is necessary to determine unambiguously the mechanism of current reduction. In terms of device performance characteristics, the main results of comparison of three types of hybrid structures can be summarized as follows: the H2 structure shows the highest short circuit current density J_{SC} = 5.87 mA/cm^2, whereas the H3 structure has the highest open circuit voltage U_{OC} = 730 mV, while both J_{SC} and U_{OC} of the H1 structure are rather low. It is worth to note that this comparison provides only some guideline for further study.

Figure 10 presents the spectral dependence of short circuit current density *J*sc (λ) for the structures H1, H2, and H3 in comparison to the solar spectral irradiance. For *J*sc (λ) form comparison, the *J*sc (λ) curves were normalized to *J*sc (λ) response of an a-Si:H inorganic solar cell. An interesting relative higher photo current than that for inorganic reference sample is found in the region of short wavelength from λ = 410 to 354 nm associated to the frontal interface of the structures. It suggests better electronic properties of organic-inorganic frontal interfaces due to lower surface back diffusion coefficient of carriers generated close to this interface or/and lower surface recombination rate and probably more stable chemical interface [28]. Some confirmation on quality of undoped absorber material can be obtained from subgap for $h\nu < E_{opt}$ photocurrent. Slope of $J_{SC}(h\nu)$ characterized by E_0 in the vicinity of E_{opt} is approximately the same in the all structures meaning that the organic semiconductor has narrow band tail density of states. As far as deep states are concerned, the sample H1 shows the highest value, sample H2 higher value than that in the reference sample, but less than that in H1 sample. In the sample H3 was not able to measure signal for $h\nu$ < 1.6 eV. In other words, quality of nondoped absorber with organic semiconductor is still less than that for Si:H films that motivates further efforts in improvement of electronic properties of organic semiconductors.

Some sort of "optimization" (see details in [28]) has been performed for H2 type of structure. **Figure 11** shows the current voltage characteristics of an improved hybrid H2* structure in comparison to those for organic and inorganic solar cells. It is most interesting that J_{SC} = 17.7 mA/cm^2 value exceeds values for both reference samples (organic and inorganic Si:H p-i-n structure). This high value may result from: (a) higher electric field at the frontal interface PEDOT/PSS-i-Si:H, and consequently reducing back diffusion and increasing current, (b) reducing surface recombination rate at the interface, and (c) better electronic quality of Si:H film grown on PEDOT/PSS. Though the latter cannot be excluded, no experimental evidence on changes electronic properties of Si:H film in this structure. U_{OC} = 645 mV for this H2* structure is higher than that for organic and less than that for Si:H p-i-n structure. At low voltage in the vicinity of U_{OC}, photocurrent is suppressed indicating high transversal leakage current. Finally, the comparison of performance characteristics for H2* structure reported for PEDOT/(i) Si:H/(n) Si:H devices is performed (see **Table 3**). H2 structure demonstrates a large high value of short circuit current density J_{SC} = 17.7 mA/cm^2 in H2* structures, this makes promising further study of this kind of photovoltaic cell, especially if the transversal leakage current is significantly reduced.

http://dx.doi.org/10.5772/67565

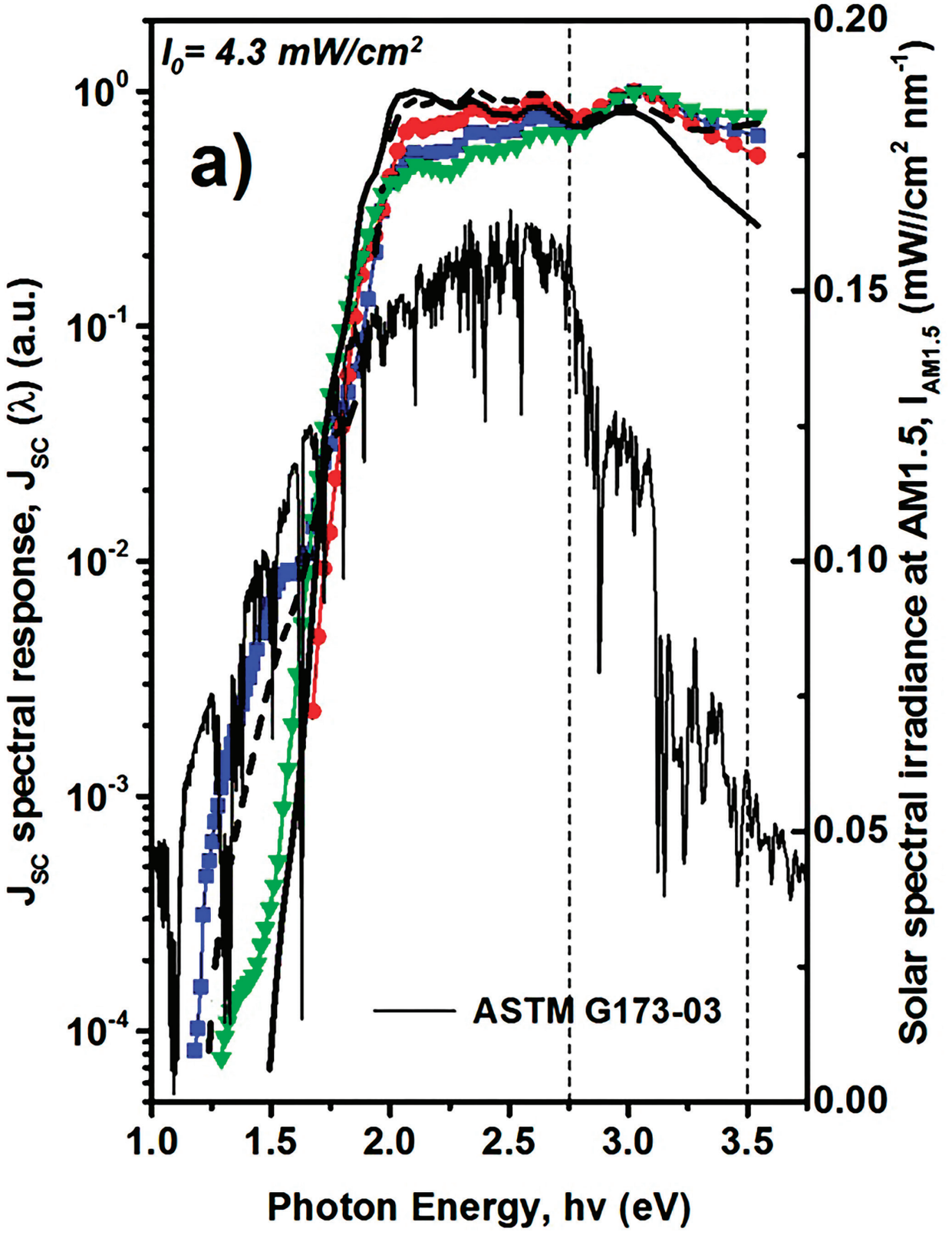

Figure 10. Spectral dependence of short circuit current density in the structures H1, H2, and H3 in comparison with solar spectral irradiance.

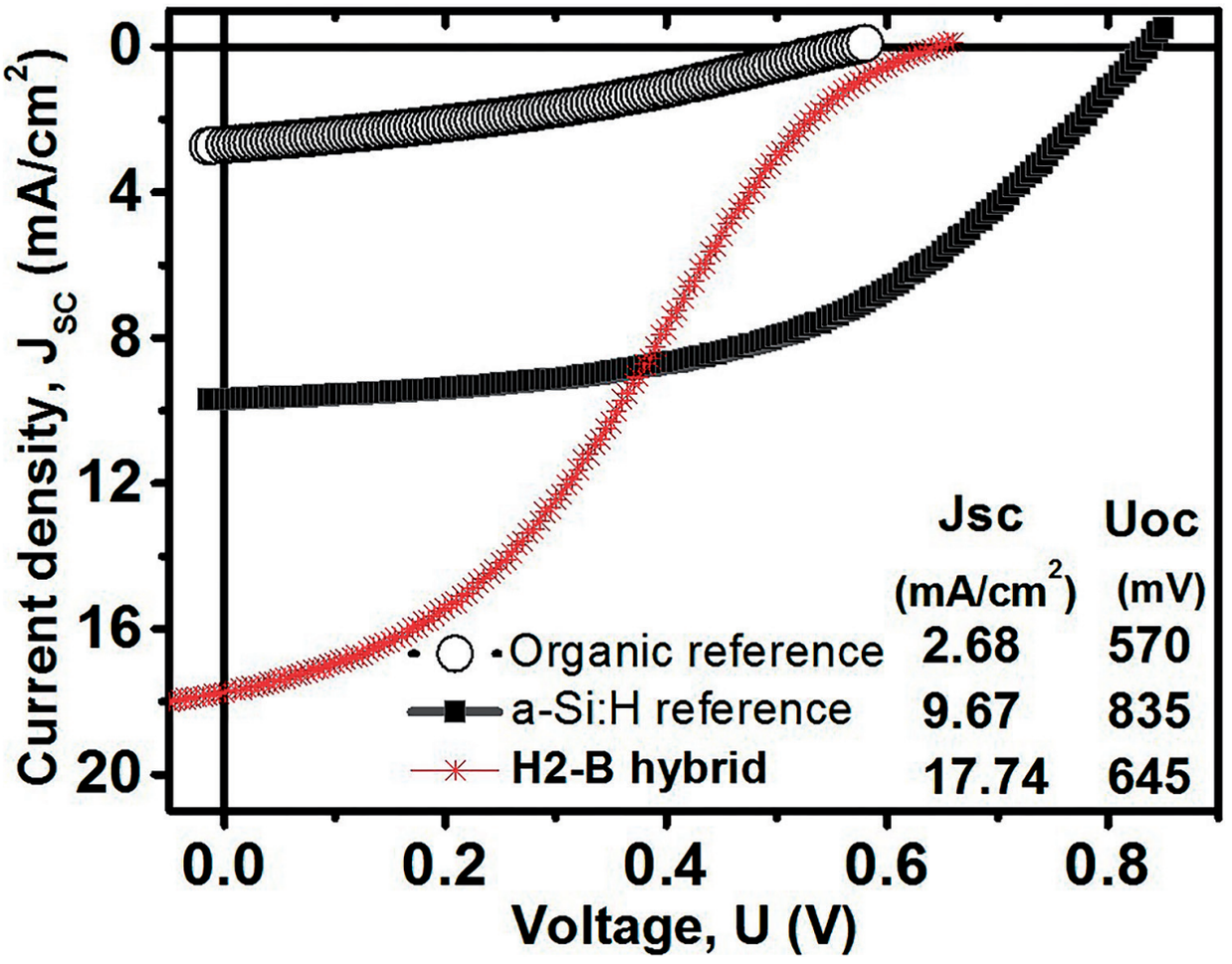

Figure 11. Current-voltage characteristics $J(U)$ and extracted U_{OC}, J_{SC}, FF and conversion efficiency values for hybrid photovoltaic structures in H2* configuration, organic, and inorganic reference solar cells.

Frontal interface	J_{SC} (mA/cm^2)	U_{OC} (V)	FF	PCE (%)
PEDOT:PSS/(i)a-Si:H	4.55	0.88	51	2.1
	16.0	0.54	50	4.7
	17.74	0.64	32	3.75
a-SiC:H:B/(i) a-Si:H efficiency record	16.36	0.89	71	10.2

Table 3. Comparison of PV characteristics reported in literature with the best structure (H2) PEDOT:PSS/Si:H [28].

5. Hybrid structures on flexible substrates

Flexible solar cells on plastic substrates have several advantages such as lightweight and relative low cost. Inorganic and organic semiconductor technologies have demonstrated to be compatible with flexible substrates [12, 33–35]. However, the new concept of hybrid PECVD-polymer solar cell on flexible substrates has not been reported until now. A hybrid solar cell ((AZO/PEDOT:PSS/

http://dx.doi.org/10.5772/67565

(i) Si:H/(n) Si:H//Ag) on PEN and polyimide substrate shown in **Figure 12** have been fabricated and studied. A transparent electrode of AZO was deposited on the flexible substrate by sputtering method. The inorganic silicon layers were deposited by RF PECVD process at substrate temperature of T_d = 160°C and Ag top contact was deposited by sputtering at the same temperature and the PEDOT:PSS film was deposited by spin coating. A reference structure was fabricated on Corning glass substrate and demonstrated a *J*sc = 10.4 mA/cm^2 and *V*oc = 565 mV.

Similar structures on PEN with different AZO-film thickness were compared; it was found that the performance characteristics of the cell were strongly dependent on the thickness of the AZO film. The short circuit current density increased from *J*sc = 3.21 to 9.79 mA/cm^2 and the open circuit voltage from *V*oc = 405 to 565 mV for a AZO thickness change from *d* = 250 to 500 nm, respectively. Average roughness measured on AZO film deposited on plastic substrate as references shows a reduction from <*r*> = 1.11 nm for 250 nm thick AZO layer to <*r*> = 0.87 nm for 500 nm thick AZO layer, both on PEN substrate. Polyimide KAPTON® substrates from Du Pont™ are known for some applications such as circuits and space applications. The average roughness for 250 nm thick AZO films on polyimide show a small difference in value (1.11) in comparison to 250 nm thick AZO film on PEN substrate (1.4). The difference of average roughness between

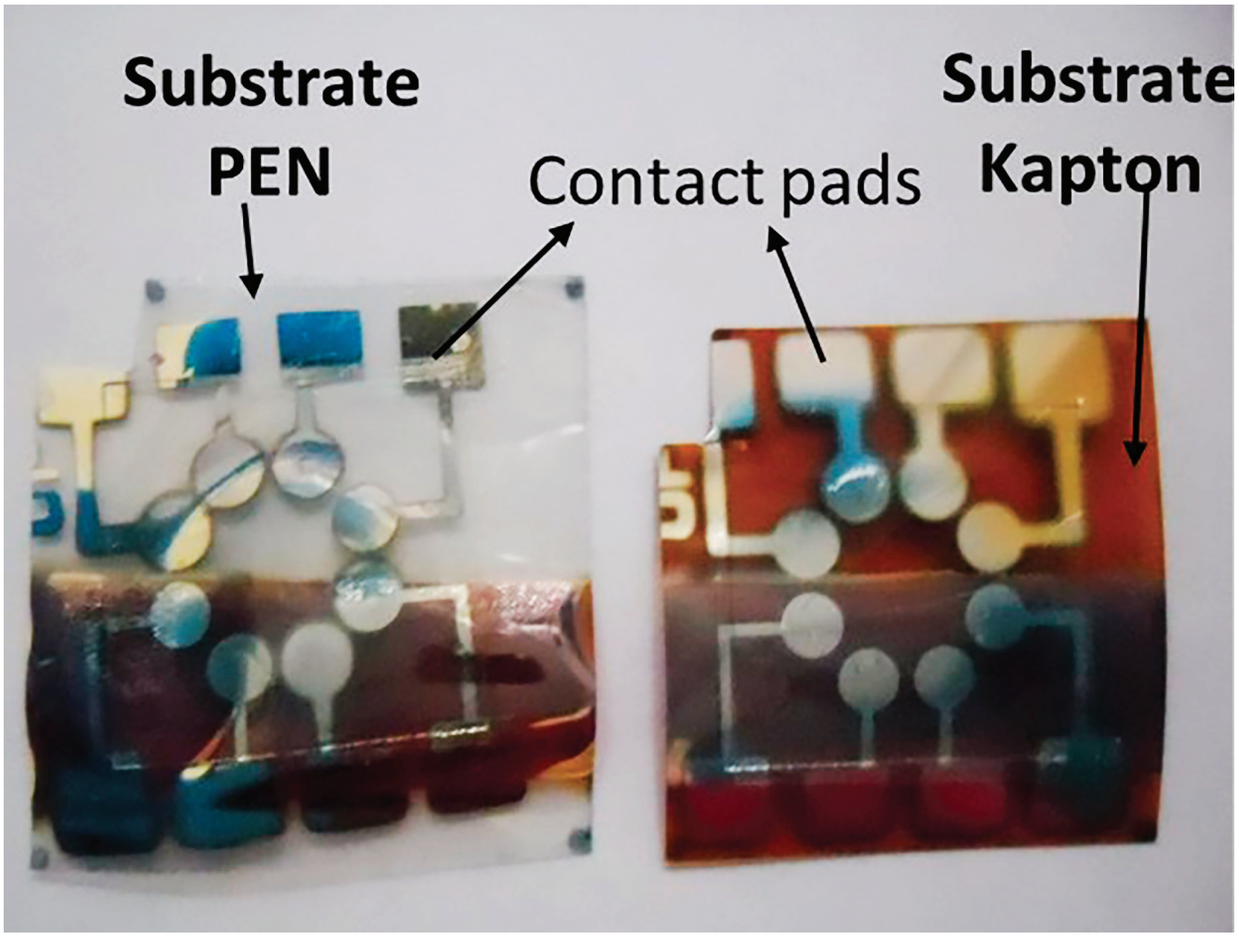

Figure 12. Hybrid photovoltaic structure on flexible substrate (PEN, left and right, KAPTON) based on Si:H and organic semiconductors PEDOT:PSS as p-type layer.

AZO on polyimide and PEN disappears for those with AZO film thickness of d = 500 nm. Polyimide has some advantages over other plastics such as high performance in electrical, chemical, and mechanical properties at relatively high temperature process of up to T = 450°C. However, its low transmission in visible range (**Figure 5**) limits implementation in solar cells. For similar solar cell structures and similar 500 nm thick AZO layer, the *J*sc reduces from 3.21 mA/cm^2 on PEN to 1.9 mA/cm^2 on polyimide because of the short wavelength limit (T < 50%) at 590 nm. The cross-sectional scanning electron microscopy (SEM) image of the solar cell on PEN is shown in **Figure 13**. The 500 nm thick AZO, 240 nm PEDOT:PSS, 300 nm thick (i) a-Si:H and 200 nm thick Ag layers and PEN substrate are well defined in the images. A large difference between the expected thickness (~45 nm) on glass substrate and PEN substrate (250 nm) was observed for PEDOT:PSS. This may be attributed to different surface properties for glass and PEN. As it can be seen, PEDOT layer looks as dispersive nonuniform material. Still it is not clear if this nonuniformity and its characteristics are intrinsic (inherent) material properties or they may depend on substrate (or previous layer) surface properties. Deviations of expected thickness and real thickness on plastic substrate were not observed for the PECVD films; however, the deformation (curvature, see **Figure 12**) of the substrates after device fabrication is an issue to be considered due to stress caused by deposition temperature and other factors in PECVD process. These curvatures are used to be the cause of misalignment effects on flexible devices. SEM images also illustrate how quality of substrate and defects of substrate are important. As we can see a defect in the substrate is transferred through all the thickness of AZO film and is

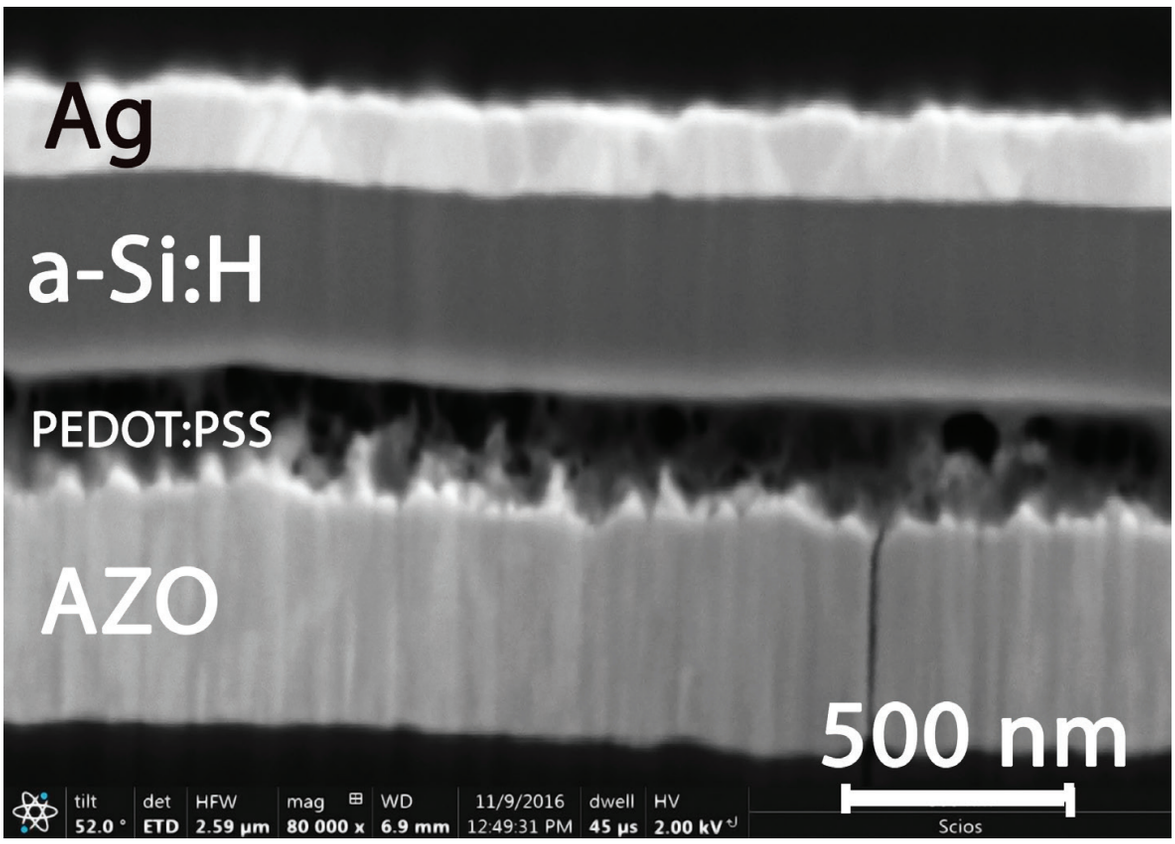

Figure 13. Hybrid solar cell cross-sectional SEM image on flexible substrate PEN/ITO/PEDOT:PSS/(i) Si:H/(n) Si:H (H2).

http://dx.doi.org/10.5772/67565

interrupted by the organic PEDOT:PSS layer. The surface quality is an important parameter that influences the final quality of the devices.

6. Summary and conclusion

In the beginning, a brief overview of polymer organic and PECVD inorganic material semiconductor technologies has been made to focus on optoelectronic characteristics and fabrication process at low substrate temperature for application on hybrid photovoltaic devices. Inorganic semiconductor materials deposited by PECVD have been reported in literature to be a mature technology compatible with large area flexible devices; while organic semiconductors and their technology are significantly less studied. On other hand, organic materials have shown potential as PV materials with several advantages in the fabrication process such as room temperature deposition and reduction of complex vacuum stages for deposition but the "ideal" process for the deposition of organic materials is still unresolved.

A concept of inorganic-organic photovoltaic devices mainly for PECVD inorganic materials has been considered. The concept is based on compatibility of both technologies and complementary electronic properties. Three types of hybrid structures have been fabricated and studied: (1) with OS as intrinsic absorber and p-, n-Si:H layers creating built-in electric field (H1 structures), (2) ITO/PEDOT:PSS/(i) Si:H/(n) Si:H structures (H2 type), and (3) structures with double intrinsic absorber such as ITO/PEDOT:PSS/P3HT:PCBM/(i) Si:H/(n) Si:H (H3). All the structures showed PV performance with different characteristics discussed and compared with those reported in the literature. Performance of the structures including those fabricated on flexible plastic substrates confirmed clear compatibility OS and PECVD technologies. The device diagnostics of the studied structures has been performed by measurements of photocurrent spectral dependencies. The measurements of subgap photocurrent revealed, that electronic quality of intrinsic OS materials, was sufficient, but worse comparing to that of Si:H films. The structures with OS frontal interfaces showed better short wavelength photocurrent response indicating better electronic properties of the interfaces comparing to reference samples. All the structures suffered from photocurrent suppression at voltages near U_{OC} values suggesting high transversal leakage current. Simple "optimization" of H2 structure resulted in substantial increase of photocurrent to the value J_{SC} = 17.7 mA/cm^2 that was higher than the values in the reference samples. Explanations of characterization data have speculative character and should be considered only as some guidelines and motivation for further study. Although some hybrid structures demonstrated substantial improvement of performance, while other hybrid structures showed poor performance, further R&D efforts seem to be promising and should be focused on deeper study of organic materials and related interface properties.

Acknowledgements

Ismael Cosme Bolaños acknowledges support from "CONACyT Cathedra" project No.2734. Hiram Enrique Martinez and Antonio Olivares acknowledge support from CONACyT through the scholarships number 362152 and 363344, respectively.

Nomenclatures

PECVD	Plasma enhanced chemical vapor deposition
CVD	Chemical vapor deposition
GD	Glow discharge
ESR	Electron-spin resonance
DOS	Density of states
LT	Low temperature
HIT	Heterojunction intrinsic thin configuration
P3HT:PCBM	Poly(3-hexythiophene):methano-fullerenephenyl-C61-butyric-acid-methyl-ester
PEDOT:PSS	Poly(3,4ethylenedioxythiophene):poly(4-styrenesulfonate)
IPA	Isopropyl alcohol
DC	Direct current
VRH	Variable range hopping
1D	One dimension
TCO	Transparent conductive oxide
PLD	Pulsed laser deposition
AZO	Aluminum zinc oxide
PET	Polyethylene terephthalate
PEN	Polyethylene naphthalate
PTFE	Polytetrafluoroethylene
CIOD	Concept for inorganic-organic device
PV	Photovoltaic
AM1.5	Air mass spectrum 1.5
SEM	Scanning electron microscopy

Author details

Andrey Kosarev[1]*, Ismael Cosme[2], Svetlana Mansurova[1], Antonio J. Olivares[1] and Hiram E. Martinez[1]

*Address all correspondence to: akosarev@inaoep.mx

1 National Institute for Astrophysics, Optics and Electronics, Optics and Electronics (INAOE), Puebla, Mexico

2 CONACyT-INAOE, Mexico

http://dx.doi.org/10.5772/67565

References

[1] J.M. Ziman, editor. Principles of the theory of solids. 2nd ed. Cambridge: Cambridge University Press; 1965. 452 p.

[2] H.F. Sterling, R.C.G. Swann. Chemical vapour deposition promoted by R.F. discharge. Solid-State Electronics. 1965;**8**:653-654.

[3] R.C. Chittick, J.H. Alexander, H.F. Sterling. The preparation and properties of amorphous silicon. Journals of Electrochemical Society. 1969;**166**:77-88.

[4] W.E. Spears, P.G. Le Comber. Substitutional doping of amorphous silicon. Solid State Communications. 1975;**17**:1193-1196.

[5] W.E. Spear, P.G. Le Comber, S. Kinmond, M.H. Brodsky. Amorphous silicon p-n junction. Applied Physics Letters. 1976;**28**:105.

[6] R. Martins, H. Aguas, V. Silva, I. Ferreira, A. Cabrita, E. Fortunato. Nanostructured silicon films produced by PECVD. Materials Research Society Symposium Proceedings. 2001;**664**:A9.6.1-A9.6.6.

[7] Y. Nasuno, M. Kondo, A. Matsuda. Passivation of oxygen-related donors in microcrystalline silicon by low temperature deposition. Applied Physics Letters. 2001;**78**:2330-2332.

[8] A. Matsuda. Formation kinetics and control of micro-crystallite in μc- Si:H from glow discharge plasma. Journal of Non-crystalline Solids. 1983;**59-60**:767-774.

[9] R. Cariou, M. Labrune, R.I. Cabarrocas. Thin crystalline silicon solar cells based on epitaxial films grown at 165°C by RF-PECVD. Solar Energy Materials and Solar Cells. 2011;**95**:2260-2263.

[10] A. Kosarev, A. Torres, C. Zuñiga, M. Adamo, L. Sanchez. Nano-structured GeySi1-y:H films deposited by low frequency plasma for photovoltaic application. Materials Research Society Symposium Proceedings. 2009;**1127**:1127-T04-03.

[11] J. Robertson. Deposition mechanism of hydrogenated amorphous silicon. Journal of Applied Physics. 2000;**87**:2608-2617.

[12] W.S. Wong, A. Salleo, editors. Flexible Electronics: Materials and Applications. 1st ed. USA: Springer Science + Business Media; 2009. 473 p.

[13] A. Terakawa. Review of thin-film silicon deposition techniques for high-efficiency solar cells developed at Panasonic/Sanyo. Solar Energy Materials & Solar Cells. 2013;**119**:204-208.

[14] Z. Mrázková, K. Postava, A. Torres-Rios, M. Foldyna, P. Roca i Cabarrocas, J. Pištora. Optical modeling of microcrystalline silicon deposited by plasma-enhanced chemical vapor deposition on low-cost iron-nickel substrates for photovoltaic applications. Procedia Materials Science. 2016;**12**:130-135.

[15] Y. Nasuno, M. Kondo, A. Matsuda. Microcrystalline silicon thin-film solar cells prepared at low temperature using PECVD. Solar Energy Materials & Solar Cells.2002;**74**:497-503.

[16] P. Alpuim, V. Chu, J.P. Conde. Amorphous and microcrystalline silicon films grown at low temperatures by radiofrequency and hot-wire chemical vapor deposition. Journal of Applied Physics. 1999;**86**(7):1.

[17] W.E. Spear, P.G. Le Comber. Electronic properties of substitutionally doped amorphous Si and Ge. Philosophical Magazine. 1976;**33**:935-949.

[18] D. Hauschildt, M. Stutzmann, J. Stuke, H. Dersch. Electronic properties of doped glow-discharge amorphous germanium. Solar Energy Materials. 1982;**8**(1-3):319-330.

[19] J. Xu, S. Miyazaki, M. Hirose. High-quality hydrogenated amorphous silicon-germanium alloys for narrow bandgap thin film solar cells. Journal of Non-Crystalline Solids. 1996;**208**(3):277-281.

[20] W.B. Jordan, B. Wagner. Effects of deposition temperature and film thickness on the structural, electrical, and optical properties of germanium thin films. MRS Proceedings. 2002;**715**:A18.2.

[21] F. Origo, P. Hammer, D. Comedi, I. Chambouleyron. The effect of ion-bombardment on the formation of voids during deposition of a-Ge:H. MRS Proceedings. 1998;**507**:477-482.

[22] A. Belfedal, Y. Bouizem, J.D. Sib, L. Chahed. Films thickness effect on structural and optoelectronic properties of hydrogenated amorphous germanium (a-Ge:H). Journal of Non-Crystalline Solids. 2012;**358**(11):1404-1409.

[23] C.-M. Wang, Y.-T. Huang, Y. Kuo-Hsi, H.-J. Hsu, C.-H. Hsu, H.-W. Zan, C.C. Tsai. Influence of hydrogen on the germanium incorporation in a-Si1-xGex:H for thin-film solar cell application. MRS Proceedings. 2010;**1245**:A04.02.1-04.02-6 .

[24] A. Kosarev, A. Torres, Y. Hernandez, R. Ambrosio, C. Zuniga, T.E. Felter, R. Asomoza, Y. Kudriavtsev, R. Silva-Gonzalez, E. Gomez-Barojas, A. Ilinski, A.S. Abramov. Silicon-germanium films deposited by low-frequency plasma-enhanced chemical vapor deposition: Effect of H2 and Ar dilution. Journal of Materials Research. 2006;**21**(1):88-104.

[25] I. Cosme. Study of GeSi:H materials deposited by PECVD at low temperatures (Td<200 °C) for device applications [thesis]. Puebla, MEX: INAOE; 2013. 157 p.

[26] C. Brabec, V. Dyakonov, U. Scherf, editors. Organic Photovoltaics. 2nd ed. Germany: Wiley-VCH Verlag GmbH & Co. KGaA; 2014. 642 p.

[27] F.C. Krebs. Fabrication and processing of polymer solar cells: A review of printing and coating techniques. Solar Energy Materials & Solar Cells. 2009;**93**:394-412.

[28] I. Cosme, A. Kosarev, S. Mansurova, A.J. Olivares, H.E. Martinez, A. Itzmoyotl. Hybrid photovoltaic structures based on amorphous silicon and P3HT:PCBM/PEDOT:PSS polymer semiconductors. Organic Electronics. 2016;**38**:271-277.

[29] K.A. Nagamatsu, S. Avasthi, J. Jhaveri, J.C. Sturm. A 12% efficient silicon/PEDOT:PSS heterojunction solar cell fabricated at <100°C. IEEE Journal of Photovoltaics. 2014;**4**(1):260-264.

[30] E.L. Williams, G.E. Jabbour, Q. Wang, S.E. Shaheen, D.S. Ginley, E.A. Schiff. Conducting polymer and hydrogenated amorphous silicon hybrid solar cells. Appl. Phys. Lett. 2005;**87**:223504-223506 .

[31] A. Olivares, I. Cosme, S. Mansurova, A. Kosarev, H.E. Martinez. Study of Electrical Conductivity of PEDOT:PSS at Temperatures >300 K for Hybrid Photovoltaic Applications. In: 12th International Conference on Electrical Engineering, Computing Science and Automatic Control (CCE); 2015; Mexico City. Mexico: CCE; 2015. p. 1-3.

[32] D. Ginley, H. Hosono, D.C. Paine, editors. Handbook of Transparent Conductors. 1st ed. Online: Springer US; 2011. 534 p.

[33] K.-H. Choi, J.-A. Jeong, J.-W. Kang, D.-G. Kim, J.K. Kim, S.-I. Na, D.-Y. Kim, S.-S. Kim, H.-K. Kim. Characteristics of flexible indium tin oxide electrode grown by continuous roll-to-roll sputtering process for flexible organic solar cells. Solar Energy Materials & Solar Cells Materials. 2009;**93**:1248-1255.

[34] H.J. Park, J.-W. Park, S.-Y. Jeong, C.-S. Ha. Transparent flexible substrates based on polyimides with aluminum doped zinc oxide (AZO) thin films. Proceedings of the IEEE. 2005;**93**(6): 1447-1450.

[35] S. Sanzaro, A.L. Magna, E. Smecca, G. Mannino, G. Pellegrino, E. Fazio, F. Neri, A. Alberti. Controlled Al3+ incorporation in the ZnO lattice at 188 °C by soft reactive co-sputtering for transparent conductive oxides. Energies. 2016;**9**:443.

[36] K. Tvingstedt, O. Inganäs. Electrode grids for ITO free organic photovoltaic devices. Advance Materials. 2007;**19**:2893-2897.

[37] J. Wu, H.A. Becerril, Z. Bao, Z. Liu, Y. Chen, P. Peumans. Organic solar cells with solution-processed graphene transparent electrodes. Applied Physics Letters. 2008;**92**:26.

[38] Y.H. Kim, C. Sachse, M.L. Machala, C. May, L. Müller-Meskamp, K. Leo. Highly conductive PEDOT:PSS electrode with optimized solvent and thermal post-treatment for ITO-free organic solar cells. Advanced Functional Materials. 2010;**94**(8):1076-1081.

[39] S.-I. Na, B.-K. Yu, S.-S. Kim, D. Vak, T.-S. Kim, J.-S. Yeo, D.-Y. Kim. Fully spray-coated ITO-free organic solar cells for low-cost power generation. Solar Energy Materials and Solar Cells. 2010;**94**(8):1333-1337.

[40] D. Alemu, H.-Y. Wei, K.-C. Ho, C.-W. Chu. Highly conductive PEDOT:PSS electrode by simple film treatment with methanol for ITO-free polymer solar cells. Energy & Environmental Sciences. 2012;**5**:9662-9671.

[41] X. Crispin, F.L.E. Jakobsson, A. Crispin, P.C.M. Grim, P. Andersson, A. Volodin, C. van Haesendonck, M. Van der Auweraer, W.R. Salaneck, M. Berggren. The origin of the high conductivity of poly(3,4-ethylenedioxythiophene) – poly (styrenesulfonate) (PEDOT–PSS) plastic electrodes. Chemistry of Materials. 2006;**18**(18):4354-4360.

[42] A. Elschner, S. Kirchmeyer, W. Lovenich, U. Merker, K. Reuter, editors. PEDOT: Principles and Applications of an Intrinsically Conductive Polymer. 1st ed. London: CRC Press; 2011. 355 p.

[43] Alshammari, A. S., Sam, F. L. M., Rozanski, L. J., Mills, C. A., Alenezi, M. R., Beliatis, M. J., Jayawardena, K. D. G. I., Underwood, J. M. and Silva, S. R. P., Controlled growth and spray deposition of silver nanowires for ITO-free, flexible, and high brightness OLEDs. Phys. Status Solidi A, 2016, DOI 10.1002/pssa.201600561

[44] A. Plichta, A. Habeck, S. Knoche, A. Kruse, A. Weber, N. Hildebrand. Flexible glass substrate. In: Crawford GP (ed), Flexible Flat Panel Displays. John Wiley & Sons Ltd, West Sussex, 2005; pp. 35-55.

[45] C.C. Wu, S.D. Theiuss, G. Gu, M.H. Lu, J.C. Sturm, S. Wagner, C.C. Wu, S.D. Theiuss, G. Gu, M.H. Lu, J.C. Sturm, S. Wagner, S.R. Forrest. Integration of organic LEDs and amorphous Si TFTs onto flexible and lightweight metal foil substrates. IEEE Electron Device Letters. 1997;**18**(12):609-612.

[46] H. Izadi, M. Golmakania, A. Penlidis. Enhanced adhesion and friction by electrostatic interactions of double-level Teflon nanopillars. Soft Matter. 2013;**9**:1985-1996.

[47] M. Wright, A. Uddin. Organic—inorganic hybrid solar cells: A comparative review. Solar Energy Materials & Solar Cells. 2012;**107**:87-111.

[48] X. Shen, B. Sun, D. Liu, S.-T. Lee. Hybrid heterojunction solar cell based on organic inorganic silicon nanowire array architecture. Journal of the American Chemical Society. 2011;**133**:19408-19415.